

Anomalous Strong Relaxation of the Polarization of Muons in the Magnetically Ordered and Paramagnetic States of the TbMnO_3 Multiferroic

D. S. Andrievskii^a, S. I. Vorob'ev^{a, *}, A. L. Getalov^a, E. I. Golovenchits^b, E. N. Komarov^a,
S. A. Kotov^a, V. A. Sanina^b, and G. V. Shcherbakov^a

^a Petersburg Nuclear Physics Institute, National Research Center Kurchatov Institute, Gatchina, 188300 Russia

^b Ioffe Institute, Russian Academy of Sciences, St. Petersburg, 194021 Russia

*e-mail: Vorobyev_SI@pnpi.nrcki.ru

Received November 21, 2016; in final form, July 7, 2017

An anomalously strong relaxation of the muon polarization in a magnetically ordered state in the TbMnO_3 multiferroic has been revealed by the μSR method below the Néel temperature (42 K). Such a relaxation is due to the muon channel of relaxation of the polarization and the interaction of the magnetic moment of the muon with inhomogeneities of the internal magnetic field of an ordered state in the form of a cycloid. Above the Néel temperature, beginning with temperatures depending on the applied magnetic field, a two-phase state has been revealed where one phase has an anomalously strong relaxation of the muon polarization for a paramagnetic state. These features of the paramagnetic state are due to short-range magnetic order domains that appear in strongly frustrated TbMnO_3 . A true paramagnetic state has been observed only at $T \geq 150\text{K}$.

DOI: 10.1134/S0021364017170052

1. INTRODUCTION

Multiferroics belong to a class of compounds where the magnetic and ferroelectric orders coexist. Of particular interest are multiferroic manganites RMnO_3 and RMn_2O_5 ($R = \text{Eu, Gd}$), where the ferroelectric order is induced by a special type of the magnetic order reducing the symmetry of a crystal to noncentrosymmetric. These multiferroic manganites exhibit a giant magnetoelectric effect, which attracts attention of researchers [1–7]. The study of features of the magnetic structure of such multiferroics is of key importance for understanding of their polar and structural states. As is known, the μSR method provides information on local internal fields of magnets in which muons stop. We previously studied the magnetic structure of RMn_2O_5 by the μSR method [8–10]. The main feature of RMn_2O_5 is the equality of the numbers of Mn^{3+} and Mn^{4+} ions; the distribution of such ions in the lattice (charge ordering) determines both the magnetic and ferroelectric properties of RMn_2O_5 [5]. We showed in [8, 9] that the relaxation properties of muons in RMn_2O_5 and in a doped $\text{Eu}_{0.8}\text{Ce}_{0.2}\text{Mn}_2\text{O}_5$ sample [10] indeed strongly depend on the spatial distribution of Mn^{3+} and Mn^{4+} ions and the charge transfer (delocalized e_g electrons) between them.

In this work, we study the relaxation of the muon polarization in TbMnO_3 . At room temperature, this

compound has an orthorhombic symmetry (space group $Pbnm$) with the lattice parameters $a = 5.3 \text{ \AA}$, $b = 5.68 \text{ \AA}$, and $c = 7.49 \text{ \AA}$ [1]. Ions Mn^{3+} are in the octahedral oxygen environment and their $3d$ shell includes three localized t_{2g} electrons and one delocalized e_g electron. The ground state of the Tb^{3+} ion (7F_6 , $S = 3$, $L = 3$) is characterized by a large magnetic moment ($J = 9\mu_B$), to which both the spin moment and orbital angular momentum contribute, and a strong spin–orbit coupling. Ions Tb^{3+} are usually described in the extremely strong anisotropic Ising approximation, which rigidly fixes the orientation of their moments in the ab plane [11].

The magnetic structure of TbMnO_3 is characterized by sinusoidal and cycloid spin states in the Mn^{3+} subsystem, as well as by ordering in the subsystem of Tb^{3+} ions coupled to the Mn^{3+} subsystem by the Tb – Mn exchange interaction. The magnetic structure was studied in detail in works on the scattering of unpolarized and polarized neutrons, as well as on X-ray resonance magnetic scattering [12]. As the temperature decreases, TbMnO_3 undergoes three phase transitions. A long-range magnetic order is established at the temperature $T_N = 42 \text{ K}$ in the form of a sinusoidal antiferromagnetic structure along the b axis. The magnetic structure of the Mn subsystem is transformed at the temperature $T_S = 28 \text{ K}$ to a spiral cycloid with

spins that rotate in the bc plane as they move along the b axis and are antiferromagnetically ordered along the c axis. The ordering of moments of Tb^{3+} ions with the same period as for the spins of Mn^{3+} ions appears simultaneously at $T \leq T_S$. In this case, the magnetic moment along the c axis appears in the Tb^{3+} subsystem [12]. Ferroelectric ordering along the c axis also appears at $T_S \approx T_{FE}$. The Tb – Tb exchange below $T_{N2} = 7$ K is responsible for a partial rearrangement of ordered Mn^{3+} and Tb^{3+} subsystems.

A TbMnO_3 polycrystalline sample was studied by the μSR method [13], but reliable results in the temperature range of the magnetically ordered state were not obtained because of methodical problems.

Using the μSR method, we studied the TbMnO_3 ceramic sample in the temperature range from 15 to 290 K. The relaxation function of the muon polarization was obtained and its parameters (asymmetry, polarization relaxation, and the precession frequency of the muon spin in the internal magnetic field of the sample) were found. The results of these studies are qualitatively different from those obtained for RMn_2O_5 and $\text{Eu}_{0.8}\text{Ce}_{0.2}\text{Mn}_2\text{O}_5$ [8–10], as well as for LaMnO_3 and $\text{La}_{1-x}\text{Ca}_x\text{MnO}_3$ manganite perovskites closest in symmetry [14, 15]. Those works were primarily focused on the relaxation of the muon polarization below the magnetic ordering temperature and the paramagnetic state was a normal single-phase state with a weak relaxation of the polarization. Strong narrow maxima of the relaxation rate were observed near the transition temperature T_N . The separation into two phases with different polarization relaxation rates, which is due to phase separation (into the antiferromagnetic dielectric and conducting ferromagnetic phases) characteristic of LaAMnO_3 manganite perovskites ($A = \text{Sr}, \text{Ba}, \text{Ca}$), appeared only in doped $\text{Eu}_{0.8}\text{Ce}_{0.2}\text{Mn}_2\text{O}_5$ and $\text{La}_{1-x}\text{Ca}_x\text{MnO}_3$ samples at temperatures below $T = T_N$ [16, 17]. In this case, the ferromagnetic conducting phase had an increased relaxation rate of muon polarization.

In this work, a sharp increase in the relaxation of the muon polarization in the magnetically ordered state is detected below the temperature $T_N = 42$ K. The parameters of relaxation of the muon polarization observed in the paramagnetic phase above the temperature $T_N = 42$ K up to 150 K indicate that the state of the sample is not a normal paramagnetic state. This state can be described only under the assumption of the existence of a two-phase state of the sample, where one of the phases includes limited noninteracting magnetically ordered domains with an enhanced relaxation of the muon polarization in the internal fields of these regions. The true paramagnetic state is observed only at temperatures $T > 150$ K.

2. PREPARATION OF THE EXPERIMENT. METHOD FOR PROCESSING EXPERIMENTAL DATA

To study the TbMnO_3 sample, we used the μSR setup [18] placed at the output of the muon channel of the PNPI synchrocyclotron. Time spectra of positrons from the muon decay were measured in two time intervals (0–10 and 0–1.1 μs) with a step of 4.9 and 0.8 ns/channel, respectively.

The TbMnO_3 sample with a diameter of 30 mm and a thickness of 12 mm was manufactured in the form of a ceramic disk using the solid-phase synthesis technology. The sizes of grains in its structure was several tens of microns. The homogeneity and single-phase property of the sample were tested by X-ray phase analysis.

The measured time spectra of decay positrons were described by the expression

$$N_e(t) = N_0 \exp(-t/\tau_\mu) [1 + a_s G_s(t) + a_b G_b(t)] + B,$$

where N_0 is the normalization constant; τ_μ is the lifetime of the muon; a_s and a_b are the contributions to the observed asymmetry of positrons from the decay of muons stopped in the sample and in the construction elements of the setup, respectively; $G_s(t)$ and $G_b(t)$ are the respective relaxation functions of the muon polarization; and B is the background of random coincidences.

The background of random coincidences B was determined from the analysis of the region of the time spectrum to the time of stop of the muon in the sample (events from the sample and background events from constructive elements of the setup are absent in this region).

The parameters of the background relaxation function $G_b(t)$ from construction elements were obtained by processing the precession spectra of the muon in the external magnetic field ($H \approx 280$ G) at a certain temperature $T < T_N$:

$$G_b(t) = \exp(-\lambda_b t) \cos(\Omega_b t).$$

In this case, only the contribution from construction elements is observed at the precession frequency in the external magnetic field.

The relaxation function of the muon polarization in the sample was represented in the standard form

$$G_s(t) = G_d(t)G_{st}(t),$$

where $G_d(t) = e^{-\lambda t}$ is the dynamic relaxation function describing the effect of fluctuations of the magnetic field in the sample on the polarization of the muon during the time of its thermalization in the sample and $G_{st}(t)$ is the static relaxation function whose form and parameters are determined by the distribution of local magnetic fields in the regions of preferable localiza-

tion of the muon after its deceleration and thermalization in the sample.

The asymmetry a_s on the sample will be considered as residual; i.e., it can be different from the initial asymmetry a_0 in the paramagnetic region and this difference reflects the appearance of additional muon depolarization channels at the variation of the temperature of the sample. The parameter a_0 was determined by processing time spectra of precession obtained in the external magnetic field when the sample was in the paramagnetic state at room temperature.

The parameters of the relaxation function were found from the experimental time spectra measured in the magnetic fields $H = 0$ and 280 G.

3. RESULTS OF MEASUREMENTS AND THEIR ANALYSIS

The TbMnO₃ sample at room temperature is paramagnetic. The relaxation of the muon polarization in zero magnetic field ($H = 0$) is described by the function $G_s(t) = \exp(-\lambda t)$ with the asymmetry a_s . When a transverse external magnetic field ($H = 280$ G) is switched on, the precession of the magnetic moment of the muon is observed at the frequency $F = \gamma H \approx 3.8 \times 10^3$ kHz, where $\gamma = 13.5544$ kHz/G, obtained from the relaxation function of the muon polarization $G_s(t) = \exp(-\lambda t) \cos(\Omega t)$ with the amplitude a_0 and angular frequency $\Omega = 2\pi F$. Such a paramagnetic state of the sample holds up to $T \approx 150$ K. In this state, the precession frequency F (Fig. 1) is independent of the temperature, the relaxation rate λ remains low ($\lambda \approx 0.4 \mu\text{s}^{-1}$, see Figs. 2 and 3), and the normalized asymmetry $a_s/a_0 \approx 1.0$ holds (see Figs. 4 and 5).

At temperatures $150 \text{ K} > T > T_N$, the process of depolarization of muons cannot be adequately described by a simple relaxation function $G_s(t)$ with a single relaxation rate λ and a single asymmetry parameter. It is necessary to add a term $\sim a_2 \exp(-(\lambda_2 t)^\beta)$ to the function $G_s(t)$:

$$\begin{aligned} a_s G_s(t) &= a_1 \exp(-\lambda_1 t) \cos(\Omega_1 t) \\ &+ a_2 \exp(-(\lambda_2 t)^\beta) \cos(\Omega_2 t), \quad H \neq 0; \\ a_s G_s(t) &= a_1 \exp(-\lambda_1 t) + a_2 \exp(-(\lambda_2 t)^\beta), \\ &\beta = 1/2, \quad H = 0. \end{aligned}$$

Thus, the structure of the sample appears to be two-phase (phases $i = 1, 2$).

The parameter β for phase 2 was chosen such that the total asymmetry $a_1 + a_2$, where the parameters a_1 and a_2 are determined independently, is equal to a_0 in the entire temperature range of the existence of the

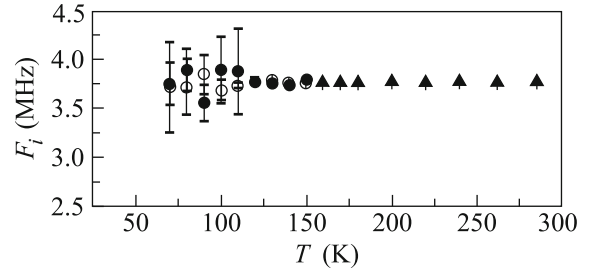


Fig. 1. Temperature dependence of precession frequencies (open circles at $T < 150$ K and triangles at $T > 150$ K) F_1 and (closed circles at $T < 150$ K and triangles at $T > 150$ K) F_2 of the magnetic moment of the muon in the external magnetic field $H = 280$ G.

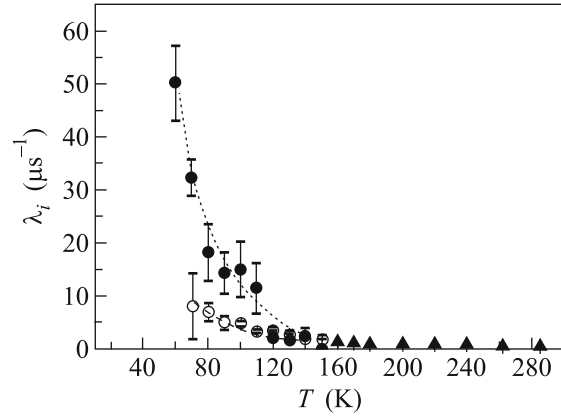


Fig. 2. Temperature dependence of the relaxation parameters (open circles) λ_1 and (closed circles) λ_2 in the external magnetic field $H = 280$ G.

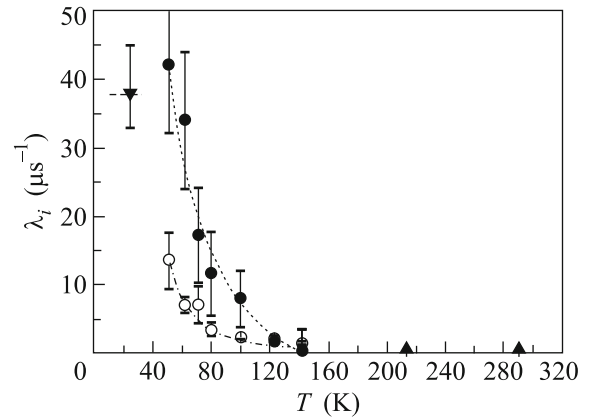


Fig. 3. Temperature dependence of the relaxation parameters (open circles) λ_1 and (closed circles) λ_2 in zero external magnetic field $H = 0$. The closed triangle corresponds to the parameter λ in the range $15 \text{ K} < T < 30 \text{ K}$.

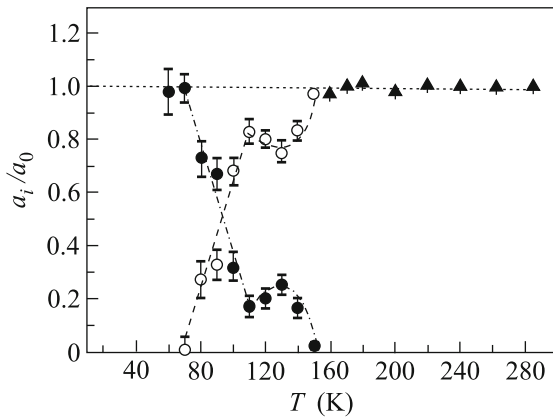


Fig. 4. Temperature dependence of normalized partial contributions (open circles at $50 \text{ K} < T < 150 \text{ K}$ and triangles at $T > 150 \text{ K}$) a_1/a_0 and (closed circles at $50 \text{ K} < T < 150 \text{ K}$ and triangles at $T > 150 \text{ K}$) a_2/a_0 to the asymmetry of decay of the muon in the external magnetic field $H = 280 \text{ G}$.

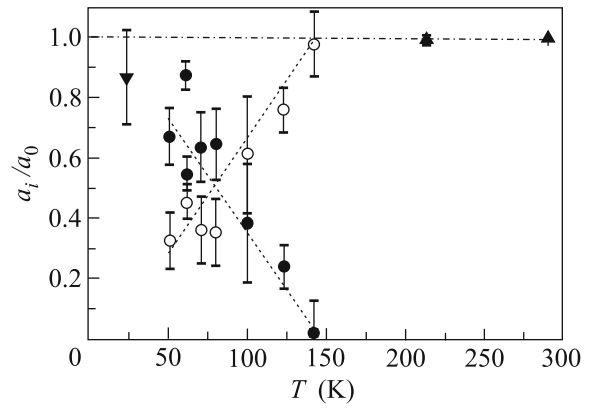


Fig. 5. Temperature dependence of normalized partial contributions (open circles at $50 \text{ K} < T < 150 \text{ K}$ and triangles at $T > 150 \text{ K}$) a_1/a_0 and (closed circles at $50 \text{ K} < T < 150 \text{ K}$ and triangles at $T > 150 \text{ K}$) a_2/a_0 to the asymmetry of decay of the muon in zero external magnetic field $H = 0$. The closed triangle corresponds to the parameter a_s in the range $15 \text{ K} < T < 30 \text{ K}$.

two-phase state. This necessary condition for the paramagnetic phase could be satisfied under the condition $\beta = 1/2$. Then, the parameters of the relaxation function of both phases are finally determined. The first terms (phase 1) have the form characteristic of the paramagnetic phase. The second phase should also be paramagnetic, but can include limited noninteracting regions with magnetic correlations. It is noteworthy that a similar expression (with the exponent $\beta = 1/2$) was used to process the μSR data for a diluted disordered magnet [19].

The phase separation of the sample into two phases at a decrease in the temperature holds down to temperatures depending on the external magnetic field (see Figs. 4 and 5). At the magnetic field $H = 280 \text{ G}$, this temperature is $T = 70\text{--}80 \text{ K}$, whereas it is noticeably lower, $T \approx 50 \text{ K}$, at zero magnetic field ($H = 0$). The relaxation rate near the lower temperature boundary of the phase coexistence is $\lambda_1 = 8\text{--}12 \mu\text{s}^{-1}$, which is much lower than $\lambda_2 = 40\text{--}50 \mu\text{s}^{-1}$. Below these boundary temperatures, only phase 2 continues to exist down to the temperature T_N ; i.e., it determines the features of the critical region near the transition. Strong relaxation of the muon polarization in the critical region indicates the appearance of unstable regions with a strong inhomogeneity of the internal magnetic field. The external field stabilizes phase 2, increases the relaxation rate λ_2 , and expands the critical region up to 70 K (see Figs. 2 and 3). Figures 4 and 5 show the temperature dependences of the normalized partial contributions to the asymmetry of the muon decay in the fields $H = 0$ and 280 G , respectively. The separation into two phases for asymmetries is observed down to the same temperatures as for relaxation rates.

It is remarkable that the relaxation rate of phase 2 is anomalously high for the paramagnetic phase and varies only slightly at the application of the external magnetic field (see Figs. 2 and 3). Consequently, the state of this phase is determined primarily by the internal field, which is much higher than the external one. Phase 2, remaining paramagnetic, most likely consists of noninteracting isolated regions with a magnetic order in the initial paramagnetic matrix. Such a state exists up to the temperature $T = 150 \text{ K}$, above which thermal fluctuations transform the state of phase 2 to a normal paramagnetic state and the parameters of phases 1 and 2 become similar to each other (see Figs. 2–5).

When the temperature of the sample decreases ($T < 150 \text{ K}$), the contributions from phases 1 and 2 to the observed asymmetry change (see Figs. 4 and 5), but the sum of these partial asymmetries in the temperature range of $50\text{--}150 \text{ K}$ does not change and is equal to the initial asymmetry a_0 . The external magnetic field leads to the appearance of correlated anomalies of asymmetries of both phases in the temperature range of $100\text{--}150 \text{ K}$ and to an increase in the temperature at which phase 1 disappears under the reduction of the temperature.

We emphasize that the condition $a_0 \approx a_1 + a_2$ cannot be ensured for TbMnO_3 within the hypothesis with two exponentials ($\sim e^{-\lambda t}$), as was accepted in [14, 15] for LaMnO_3 and $\text{La}_{1-x}\text{Ca}_x\text{MnO}_3$.

At $T \leq T_N = 42 \text{ K}$, the sample passes to a magnetically ordered state, where the relaxation function of the muon polarization has the form

$$G_s(t) = [1/3 + 2/3 \exp(-\Delta t) \cos(\Omega t)] \exp(-\lambda t).$$

Here, $\Omega = 2\pi F$ is the precession frequency of the magnetic moment of the muon in the internal magnetic field, λ is the dynamic relaxation rate of the muon polarization, and Δ is the corresponding standard deviation.

As was mentioned above, the study of this temperature range is complicated because of the strong relaxation of polarization of muons stopped in the TbMnO_3 sample and measurements were performed only at several temperatures in the range of 15–30 K. Since the parameters Δ , Ω , and λ and asymmetries a_s at $T < T_N$ usually vary only slightly at a certain distance from the critical region, we performed the joint processing of all measured spectra in the temperature range of 15–30 K and obtained the following parameters of the relaxation function averaged over this temperature range:

$$\lambda = 38 \pm 5 \mu\text{s}^{-1}, \quad \Omega = 2\pi F = 2\pi(22 \pm 0.6) \text{ MHz},$$

$$\Delta = (30 \pm 4) \text{ MHz}, \quad a_s = 0.22 \pm 0.04.$$

Figure 6 shows the relaxation functions of the muon polarization in the sample in zero external magnetic field in the temperature range of 15–30 K (lower spectrum, open circles) and at a temperature of 290 K (upper spectrum, open triangles). According to Fig. 6, the relaxation of the muon polarization remains strong in the magnetic ordering region far from the critical region.

The asymmetry obtained from the precession spectrum of the magnetic moment of the muon in the external magnetic field $H = 280$ G in the paramagnetic state of the sample ($T = 290$ K) is $a_0 = 0.252 \pm 0.006$. Since a_s and a_0 coincide with each other within the errors, it is possible to suggest that only one channel of relaxation of the muon polarization exists in the temperature range of 15–30 K and it is satisfactorily described by the relaxation function $G_s(t)$ used in processing. Using these results, one can estimate the internal magnetic field H and its spatial standard deviation Δ_H in the relaxation range of 15–30 K at the point of localization of the muon: $H = 1.62 \pm 0.04$ kG, $\Delta_H = 0.35 \pm 0.05$ kG. It is noteworthy that a very large standard deviation Δ_H indicates a large inhomogeneity of the internal magnetic field ($\Delta_H/H \approx 0.22$).

A high dynamic relaxation rate of the muon polarization in TbMnO_3 in the temperature range $T < T_N$ can be attributed to the muon channel of the polarization relaxation [20]. All Mn ions in TbMnO_3 are trivalent and each of them contains one e_g electron. In the temperature range of interest (15–30 K), the spins of Mn ions are ordered in the form of a cycloid. Such a state is formed with allowance for the Dzyaloshinskii–Morya interaction, double exchange, Hund exchange, and Jahn–Teller effect [21]. The spins of Mn^{3+} ions in the cycloid state are the same and the angle

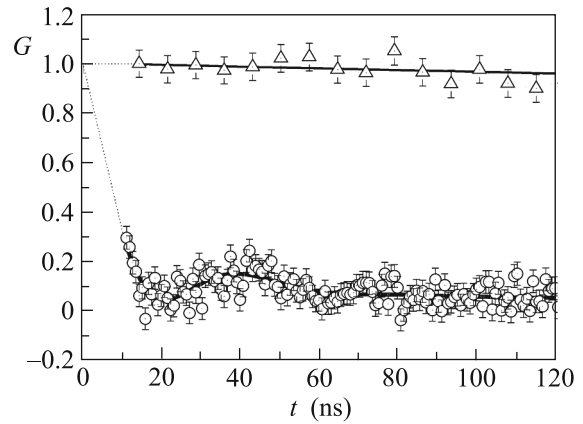


Fig. 6. Relaxation functions $G(t)$ in zero external magnetic field $H = 0$ (open triangles) at a temperature of $T = 290$ K and (open circles) in the temperature range of $T = 15$ –30 K. The dotted lines are extrapolations to the point $t = 0$ and the solid lines are simulation results.

$\theta = 0.28\pi = 50.4^\circ$ between the spins of the nearest pairs of these ions holds on the period of the cycloid [21]. The double exchange $J_{de} = t \cos(\theta/2)$, which is responsible for the transfer of e_g electrons between Mn^{3+} ions, results in the formation of muonic atoms $\text{Mu} = \mu^+ + e_g$. The transfer integral for the e_g electron is $t \approx 300$ meV [17] and $\cos(\theta/2) \approx 0.9$. Thus, the double exchange between two neighboring Mn^{3+} ions is weakened insignificantly in the cycloid as compared to the ferromagnetic state and the formation of muonium is possible.

The muonium mechanism of the muon depolarization is due to the interaction of the e_g electron of the muonium with the inhomogeneous internal magnetic field of spins of Mn^{3+} ions in the cycloid. In this case, the depolarization of the muon spin in muonium occurs through the hyperfine interaction in the muonic atom. This mechanism works for all muons stopped in the sample. The frequency of the hyperfine splitting in the free muonic atom is $\nu_0 = \omega_0/2\pi \approx 4.46 \times 10^9$ Hz [22]. The characteristic frequency for double exchange $J_{de} \approx 270$ meV is $\nu = 6.6 \times 10^{13}$ Hz. The stochastic change in the spin projection of the electron is transferred to the spin of the muon in muonium if $\nu \leq \nu_0$ [22]. In the case of fast exchange, when $\nu \gg \nu_0$, the hyperfine coupling in muonium breaks. In this case, the spins of muons directly interact with stochastic internal magnetic fields of the cycloid, which are responsible for the measured quite large transverse component of the relaxation function (large standard deviation Δ). A high frequency of the reorientation of spins of e_g electrons at the appearance and disappearance of the

hyperfine interaction in muonium is responsible for the exponential relaxation of the longitudinal muon polarization. The following expression was obtained in [20, 22] for the relaxation rate of the longitudinal component λ at $v \gg v_0$:

$$\lambda = (\omega_0^*)^2 / 4v,$$

where ω_0^* is the frequency of the hyperfine splitting of muonium in the medium and v is the frequency of the reorientation of the electron spin in muonium. The frequency of the hyperfine splitting in the medium ω_0^* can be lower than the vacuum value, but we set $\omega_0^* = \omega_0$ for an estimate. The experimental value $\lambda = 38 \mu\text{s}^{-1}$ gives the frequency $v = 5.2 \times 10^{12}$ Hz. This frequency is lower than the characteristic value $v = 6.6 \times 10^{13}$ Hz for double exchange because some muons form the transverse component of the relaxation function. Thus, the observed strong longitudinal relaxation of muons in the spin cycloid state in TbMnO_3 can really be attributed to a high frequency of reorientation of the spins of e_g electrons in muonium with allowance for double exchange.

A high relaxation rate in both the magnetically ordered and near paramagnetic ranges is remarkable (see Figs. 2 and 3). It indicates the similarity of the internal magnetic fields determining the parameters of the relaxation function. At $T > T_N$, short-range order domains apparently have symmetry close to that existing in the ordered state. The short-range order appears because of frustrations of the magnetic state of TbMnO_3 . Such frustrations can be attributed to the competition between the main interactions responsible for the magnetic state of TbMnO_3 [5, 6]. The competition of the ferromagnetic exchange interaction between the nearest neighbor spins of Mn^{3+} ions in the ab plane with the antiferromagnetic interaction between the next-nearest spins in the same plane is responsible for the noncollinear antiferromagnetic structure in the temperature range of 29–42 K [21].

It is noteworthy that studies of the temperature dependence of the magnetization of TbMnO_3 single crystals in the magnetic field ($\mathbf{H} \parallel c$, $H = 1$ kG) revealed an anomaly in the form of a small wide maximum in the temperature range of 60–150 K [23]. This anomaly was the most pronounced only along the c axis of the crystal, for which the prevailing contribution of the magnetic moments of Tb^{3+} ions is absent. The authors of [23] mentioned that the Curie–Weiss law is invalid in TbMn_2O_5 up to a temperature of 150 K. Coexisting phases 1 and 2 in the paramagnetic region in which the relaxation of the muon polarization occurs in different ways can be interpreted as follows. Phase 1 is a paramagnetic state of single Mn and Tb ions. We attribute noninteracting local domains with the short-range magnetic order located inside phase 1 to phase 2. The observed temperature depen-

dences of the asymmetries of phases 1 and 2 (see Fig. 4 and 5) reflect the relation between these phases for different temperatures and magnetic fields. As a result, the relation between these phases is unity at comparatively high temperatures depending on the external field: $T = 80$ K ($H = 0$) and $T = 93$ K ($H = 280$ G). Phase 2 prevails below the indicated temperatures down to T_N . As the temperature T_N is approached, the sizes of short-range order domains increase and the internal fields in them approach the field in the ordered domain.

We attribute the anomalies of the asymmetries of phases 1 and 2 in the temperature range of 100–150 K to the effect of the applied magnetic field $H = 280$ G on short-range order domains (see Fig. 4). These anomalies are absent in zero external field (see Fig. 5). The sizes of short-range order domains decrease with an increase in the temperature above the temperature T_N . Magnetizing fields for short-range order domains are the internal field of anisotropy of Tb^{3+} ions and the external field. The internal field decreases sharply with an increase in the temperature because of a decrease in the magnetization of Tb ions, which leads (at $H = 0$) to linear antiphase temperature variations of the asymmetries of two phases (see Fig. 5). The internal field becomes equal to the external field near a temperature of 100 K. The latter field begins to exceed the anisotropy field up to 150 K (i.e., to the boundary of the existence of the two-phase state). The manifestation of the anomaly of the magnetization along the c axis in the TbMnO_3 single crystal in the field $H = 1$ kG in [23] begins with a temperature of 60 K.

4. CONCLUSIONS

The μSR study of the TbMnO_3 ceramic sample has revealed a number of features that were not yet observed in previously studied multiferroic manganites RMn_2O_5 and LaMnO_3 -type manganite perovskites. A single-phase magnetically ordered state with an anomalously strong relaxation of the muon polarization exists below the temperature $T_N = 42$ K. Such a relaxation is due to the muon channel and to the direct interaction of the magnetic moment of the muon with inhomogeneities of the internal magnetic fields in the cycloidal ordering state.

At $T > T_N$, we have revealed a two-phase state that exists in a temperature range depending on the applied magnetic field. Because of the frustration of the magnetic state of TbMnO_3 at a temperature of $T \geq T_N$, there is a wide temperature range of existence of short-range order domains constituting a rapidly relaxing phase, where the relaxation rate is comparable with that at $T \leq T_N$. The second phase of the paramagnetic state is a normal paramagnetic phase. There is a wide temperature range of the critical state near the temperature T_N , which in fact coincides with the range of

existence of short-range order domains. As the temperature increases, thermal fluctuations destroy short-range order domains. A true paramagnetic state appears only at $T > 150$ K.

REFERENCES

1. T. Kimura, T. Goto, H. Shintani, K. Ishizaka, and Y. Tokura, *Nature (London)* **426**, 55 (2003).
2. N. Hur, S. Park, P. A. Sharma, J. S. Ahn, S. Guba, and S.-W. Cheong, *Nature (London)* **429**, 392 (2004).
3. H. Katsura, N. Nagaosa, and A. V. Balatsky, *Phys. Rev. Lett.* **95**, 057205 (2005).
4. M. Mostovoy, *Phys. Rev. Lett.* **96**, 067601 (2006).
5. I. A. Sergienko, C. Sen, and E. Dagotto, *Phys. Rev. Lett.* **97**, 227204 (2006).
6. I. A. Sergienko and E. Dagotto, *Phys. Rev. B* **73**, 0944345 (2006).
7. J. van den Brink and D. J. Khomskii, *J. Phys.: Condens. Matter* **20**, 434217 (2008).
8. S. I. Vorob'ev, E. I. Golovenchits, V. P. Koptev, E. N. Komarov, S. A. Kotov, V. A. Sanina, and G. V. Shcherbakov, *JETP Lett.* **91**, 512 (2010).
9. S. I. Vorob'ev, A. L. Getalov, E. I. Golovenchits, E. N. Komarov, V. P. Koptev, S. A. Kotov, I. I. Pavlova, V. A. Sanina, and G. V. Shcherbakov, *Phys. Solid State* **55**, 466 (2013).
10. S. I. Vorob'ev, D. S. Andrievskii, S. G. Barsov, A. L. Getalov, E. I. Golovenchits, E. N. Komarov, S. A. Kotov, A. Yu. Mishchenko, V. A. Sanina, and G. V. Shcherbakov, *J. Exp. Theor. Phys.* **123**, 1017 (2016).
11. K. P. Belov, A. K. Zvezdin, A. M. Kadomtseva, and R. Z. Levitin, *Orientation Transitions in Rare-Earth Magnetism* (Nauka, Moscow, 1979) [in Russian].
12. N. Aliouane, O. Prokhorenko, R. Feyerherm, M. Mostovoy, J. Strempler, K. Habicht, K. C. Rule, E. Dudzik, A. U. B. Wolter, A. Maljuk, and D. N. Argyriou, *J. Phys.: Condens. Matter* **20**, 434215 (2008).
13. A. A. Nugroho, Risdiana, N. Mufti, T. T. M. Palstra, I. Watanabe, and M. O. Tjia, *Physica B* **404**, 785 (2009).
14. R. H. Heffner, J. E. Sonier, D. E. MacLaughlin, G. J. Nieuwenhuys, G. Ehlers, F. Mezei, S.-W. Cheong, J. S. Gardner, and H. Roder, *Phys. Rev. Lett.* **85**, 3285 (2000).
15. R. H. Heffner, J. E. Sonier, D. E. MacLaughlin, G. J. Nieuwenhuys, G. M. Luke, Y. J. Uemura, W. Ratcliff, S. W. Cheong, and G. Balakrishnan, *Phys. Rev. B* **63**, 094408 (2001).
16. M. Yu. Kagan and K. I. Kugel', *Phys. Usp.* **44**, 553 (2001).
17. L. P. Gor'kov, *Phys. Usp.* **41**, 589 (1998).
18. S. G. Barsov, S. I. Vorob'ev, V. P. Koptev, E. N. Komarov, S. A. Kotov, and G. V. Shcherbakov, *Instrum. Exp. Tech.* **50**, 750 (2007).
19. O. Ofer, J. Sugiyama, J. H. Brewer, E. J. Ansaldo, M. Mansson, K. H. Chow, K. Kamazawa, Y. Doi, and Y. Hinatsu, *Phys. Rev. B* **84**, 054428 (2011).
20. A. N. Belemuk, Yu. M. Belousov, and V. P. Smilga, *J. Exp. Theor. Phys.* **84**, 402 (1997).
21. S. Picozzi, K. Yamauchi, I. A. Sergienko, C. Sen, B. Sanyal, and E. Dagotto, *J. Phys.: Condens. Matter* **20**, 434208 (2008).
22. V. P. Smilga and Yu. M. Belousov, *Muon Method for the Study of Matter* (Nauka, Moscow, 1991) [in Russian].
23. I. V. Golosovsky, A. A. Mukhin, V. Yu. Ivanov, S. B. Vakhrushev, E. I. Golovenchits, V. A. Sanina, J.-U. Hoffmann, R. Feyerherm, and E. Dudzik, *Eur. Phys. J. B* **85**, 103 (2012).

Translated by R. Tyapaev